

## Morphological analysis of *Chlamydia pneumoniae*

Naoyuki Miyashita<sup>1)</sup>, Akira Matsumoto<sup>2)</sup>, Rinzo Soejima<sup>3)</sup>, Toshio Kishimoto<sup>1)</sup>,  
Masamitsu Nakajima<sup>1)</sup>, Yoshihito Niki<sup>1)</sup> and Toshiharu Matsushima<sup>1)</sup>

Division of Respiratory Diseases, <sup>1)</sup>Department of Medicine and <sup>2)</sup>Department of Microbiology,  
Kawasaki Medical School, Matsushima 577, Kurashiki city, Okayama 701-01, Japan

<sup>3)</sup>Division of Welfare, Kawasaki University of Medical Welfare

(Received February 18, 1997 · Accepted March 19, 1997)

In recent years we have succeeded in isolating 18 strains of *Chlamydia pneumoniae* strains, which we designated KKpn-1~KKpn-18, from the nasopharynx of patients with acute respiratory tract infections. In the present study, we examined the morphology of these clinical isolates and compared their morphology with that of *C. pneumoniae* TW-183, AR-39, AR-388 (TWAR), IOL-207, Kajaani-6, YK-41, *Chlamydia psittaci* Frt-Hu/Cal 10, *Chlamydia trachomatis* L2/434/Bu and *Chlamydia pecorum* Bo/E58. The results indicated that the "pear-shape" of the elementary body (EB) is not a valid morphological criterion for recognizing a member of *C. pneumoniae*, although the basic morphological properties, such as location of the nucleus, presence of projections on the surface of the organisms, and the dimension of hexagonally arrayed regular structures on the inner surface of the EB outer membrane, were similar in all members of the genus *Chlamydia*. It was, therefore, concluded that the morphology of the KKpn-1~KKpn-18 strains was identical to that of *C. trachomatis*, *C. psittaci* and *C. pecorum* organisms, and that the EB profiles are different from those of *C. pneumoniae* TWAR strains.

**Key words:** *Chlamydia pneumoniae*, pear- or round-shaped EB, Button structure, surface projection, hexagonal structure

### Introduction

The chlamydiae, obligate intracellular parasites, have been assigned to a single genus, *Chlamydia*, which comprises four species, *Chlamydia pneumoniae*<sup>1)</sup>, *Chlamydia trachomatis*<sup>2)</sup>, *Chlamydia psittaci*<sup>2)</sup> and *Chlamydia pecorum*<sup>3)</sup>. These organisms multiply through a common, unique developmental cycle in which there are two morphologically and functionally distinct forms: one is the infectious elementary body (EB) and the other is the reproductive reticulate body (RB). The EB penetrates a susceptible host cell by being phagocytized and is converted into an RB, which multiplies by binary fission. The RB then undergoes maturation through an intermediate body, to form a mature progeny EB<sup>4)</sup>.

*C. pneumoniae* is well recognized as a major respiratory pathogen<sup>5)</sup>. The organism is a common cause of pneumonia, bronchitis, sinusitis, and pharyngitis, as well as being responsible for up to 10% of cases of community-acquired pneumonia<sup>6,7)</sup>. The prevalence of *C. pneumoniae* infections has a worldwide status sim-

ilar to that of *C. trachomatis* infections<sup>8)</sup>. In addition, recent investigations have suggested a possible association of *C. pneumoniae* infection with atherosclerotic cardiovascular disorders<sup>8,9)</sup>, acute exacerbations of chronic obstructive pulmonary disease<sup>10,11)</sup>, and bronchial asthma<sup>12,13)</sup>.

In the last four years, we succeeded in isolating 18 *C. pneumoniae* strains, designated KKpn-1~KKpn-18<sup>11,14,15)</sup>, from the nasopharynx of patients with acute respiratory tract infections. In the present study, we examined the morphology of the clinical isolates (KKpn-1~KKpn-18) and compared it with the morphology of established strains of *C. pneumoniae*, *C. trachomatis*, *C. psittaci* and *C. pecorum*.

### Materials and Methods

#### Chlamydial strains

The following chlamydial strains were used: *C. pneumoniae* TW-183, AR-39, AR-388<sup>7)</sup>(TWAR), IOL-207<sup>16)</sup>, Kajaani-6<sup>17)</sup>, YK-41<sup>18)</sup>, KKpn-1<sup>15)</sup>, KKpn-15<sup>14)</sup>, KKpn-16<sup>11)</sup> and 15 clinical isolates<sup>15)</sup>, *C. psittaci* Frt-Hu/Cal 10<sup>19)</sup>; *C. trachomatis* L2/434/Bu<sup>20)</sup>

and *C. pecorum* Bo/E58<sup>21)</sup> strains. Strains TW-183, AR-39 and AR-388 were purchased from the Washington Research Foundation, Seattle, WA, USA. Strains IOL-207 and Kajaani-6 were supplied by P. Saikku, University of Helsinki, Finland. Strain, YK-41 was supplied by Kanamoto Y, Hiroshima Prefectural Institute of Public Health, Japan. KKpn-1, KKpn-15, KKpn-16 and 15 other clinical isolates of the *C. pneumoniae* strains were isolated in our own laboratory. These *C. pneumoniae* strains were grown in HeLa 229 or HL cell cultures and harvested on day 3 postinoculation. *C. pecorum* E58 was supplied by Hirai K, Faculty of Agriculture, Gifu University. *C. trachomatis* L2 was supplied by Yamasaki S, National Institute of Health, Japan. *C. psittaci* Cal 10 has been maintained in our laboratory for more than 20 years. *C. trachomatis* L2 and *C. psittaci* Cal 10 were grown in L929 suspension or monolayer cultures and HeLa 229 cell cultures and then harvested on day 2 or 3 postinoculation. *C. pecorum* E58 was propagated continuously in a MDBK cell line.

#### Cultivation of infected cells in the experiments

HeLa 229 cells were used for infection with *C. pneumoniae* strains. After brief sonication, all inocula were centrifuged ( $900 \times g$  for 60 min at room temperature) onto the cell monolayers. Infected cells were then incubated at  $35^\circ\text{C}$  in an atmosphere of 5%  $\text{CO}_2$  in minimum essential medium (MEM, Nissui, Tokyo) containing  $1 \mu\text{g}/\text{ml}$  cycloheximide and supplemented with 10% heat-inactivated fetal calf serum. The Cal 10 and L2 strains were inoculated onto L929 cells without centrifugation. Similarly, MDBK monolayer cells were inoculated with the E58 strain and then incubated at  $37^\circ\text{C}$  in an atmosphere of 5%  $\text{CO}_2$  in Dulbecco-modified MEM (Nissui, Tokyo) supplemented with 10% serum.

#### Light microscopy

To examine the morphology and stainability of the intracytoplasmic inclusions, a monolayer of L929 cells or HeLa 229 cells on a cover slip (14 mm in diameter) was inoculated and incubated as described above. After incubation for 48~72 h, the infected cells were air-dried, fixed in absolute methanol, and stained with iodine and May-Gruenwald-Giemsa staining solutions. The cells were also fixed with absolute ethanol and stained with *C. pneumoniae* species-specific monoclonal antibodies (MAbs), RR-402 (Washington Research Foundation, Seattle, USA)<sup>22)</sup> and SCP-53<sup>23)</sup>, *C. trachomatis* species-specific MAb,

MicroTrak (Syva Co.), genus-specific MAb, Cultureset (Ortho Diagnostics Systems, Inc.) and XC-60, which was obtained in our laboratory and confirmed to be an MAb directed to the species-specific epitope of *C. pneumoniae* 60 kDa heat-shock protein<sup>14)</sup>.

#### Preparation of EBs

EBs of the *C. psittaci* and *C. pecorum* strains were purified by the method of Tamura and Higashi<sup>24)</sup>. Our preliminary experiments indicated that EB preparations of *C. pneumoniae* and *C. trachomatis* strains purified by the method of Tamura and Higashi<sup>24)</sup> or Caldwell et al.<sup>25)</sup> contained a number of RBs and their fragments. We therefore established a new method for the purification of *C. pneumoniae* and *C. trachomatis* EBs<sup>26)</sup>. At 72 h postinoculation, infected cells were collected in sucrose-phosphate-glutamate solution (SPG: sucrose 7.5%,  $\text{KH}_2\text{PO}_4$  0.052%,  $\text{Na}_2\text{HPO}_4 \cdot 2 \text{H}_2\text{O}$  0.1529%, glutamic acid 0.072%) and homogenized with a Teflon homogenizer. After brief centrifugation at  $900 \times g$  for 10 min at room temperature to remove cell debris, the supernatant obtained was layered onto a two-layer cushion (bottom layer, 50% wt/vol sucrose solution; top layer, 30% vol/vol Urografin [3,5-diacetamido-2,4,6-triisobenzoic acid; Schering AG, Berlin/Bergkamen, Germany] in 30 mM Tris-HCl buffer [pH 7.3]); and then centrifuged at  $8,000 \times g$  for 60 min at  $4^\circ\text{C}$  with an RPS-25 swing rotor (Hitachi, Tokyo, Japan). The precipitate and the turbid bottom layer were suspended together in SPG and centrifuged at  $12,000 \times g$  for 30 min at  $4^\circ\text{C}$ . The precipitate obtained was suspended in SPG and then treated with DNase and RNase (final concentration;  $20 \mu\text{g}/\text{ml}$  each) for 30 min at  $37^\circ\text{C}$ . The suspension was layered onto a continuous Urografin gradient column (40 to 52% vol/vol) and centrifuged at  $8,000 \times g$  for 60 min at  $4^\circ\text{C}$ . Two distinct bands were formed in the gradient column. The presence of a number of complete EBs was confirmed the lower band by electron microscopy. After washing with SPG, the EBs were suspended in SPG and stored at  $-70^\circ\text{C}$  until required.

#### Preparation of EB outer membranes

Four milliliters of purified EB suspension in Tris buffer was mixed with 6g of glass beads (0.1 mm in diameter; M and S Instruments Inc., Osaka, Japan) and shaken vigorously on a Cell Mill shaker (Edmund Bühler, Tübingen, Germany) at 70 CPS for 4 min. After centrifugation at  $10,000 \times g$  for 60 min at  $4^\circ\text{C}$  on

a sucrose cushion (sucrose 15% wt/vol), the precipitate was recovered in 0.2 M Tris-HCl buffer (pH 7.4) containing MgCl<sub>2</sub> 5 mg/ml and treated with a mixture of DNase and RNase (final concentration; 20 µg/ml each) at 37°C for 60 min. This was followed by trypsin treatment (50 µg/ml) at 37°C for 60 min and finally with 0.125% sodium dodecylsulfate (SDS) at 37°C for 10 min to remove the inner membranes. After washing twice, the insoluble outer membranes were suspended in distilled water and stored at -70°C until required.

### Electron microscopy

To examine the morphology of the organisms *in situ*, infected cells were collected at 24, 48 and 72 h postinoculation by brief centrifugation (300 × g for 3 min) and doubly fixed with 2.5% glutaraldehyde in 0.1 M cacodylate buffer (pH 7.3) for 60 min and 2.5% OsO<sub>4</sub> in the same buffer for 60 min. Thin sections were prepared and examined as reported previously<sup>27</sup>.

For shadow-casting, EBs or outer membranes were mounted on a specimen grid and coated with platinum-palladium in a vacuum shadower<sup>28</sup>. For negative staining, outer membranes were mounted on a carbon-covered grid and placed onto a droplet of 1% phosphotungstic acid (PTA, pH 7.3) solution. To prepare freeze-replicas, infected cells were pelleted by centrifugation, fixed with 2.5% glutaraldehyde, and then impregnated with 40% glycerol to prevent morphological damage by ice crystal formation. After freezing in liquid nitrogen, replicas were prepared in a Balzers 3AF 301 freeze-replica apparatus as described previously<sup>29</sup>.

The specimens were examined with a Hitachi H-500 or JEM-2000 transmission electron microscope at 75 or 80 kV.

To observe projections on the surface of *C. pneumoniae* EBs, the purified EBs were mounted on a nickel grid without a supporting membrane and doubly fixed with the glutaraldehyde and OsO<sub>4</sub> fixatives. The specimens were additionally treated with 2% tannic acid to stabilize the morphology of the projections, as reported previously<sup>30</sup> and then dehydrated in an ethanol series, dried in a Hitachi HCP-1 critical point dryer, followed by coating with Pt-palladium alloy in a Hitachi E-102 Ion Sputter unit. The specimens were examined with a Hitachi S-570 scanning electron microscope at 25 kV.

To determine the location of lipopolysaccharide

(LPS) on the EB surface of all strains, immunogold labeling was performed by the method of Birkelund et al.<sup>31</sup>. Briefly, the specimen was mounted on a grid covered with a collodion membrane and exposed to anti-LPS MAb (supplied by Hirai K, Faculty of Agriculture, Gifu University, Gifu, Japan), washed with phosphate-buffered-saline, and then mixed with a suspension of protein A-gold particles (15nm in diameter, Amersham Co.). After several washings, the specimen was examined with the Hitachi H-500 transmission electron microscope at 75 kV.

### Determination of the spacing of regular structure by Fourier transformation

To determine the spacing of the hexagonal regular structure in the EB outer membrane, diffraction images were obtained by a formula programmed in an IBAS 2000 image analysis system (Zeiss, Germany)<sup>32</sup>. Briefly, the information in a micrograph was in put into the image memory of the system through a camera, and the Fourier integral was calculated in the computer system, so that the original image in the micrograph was displayed as a diffraction pattern. The average spacing of the regular structure was calculated by measuring of the distance from the origin of the transform (frequency 0) to the diffraction spots. In some cases, the images were reconstituted from the selected spots in the diffraction pattern by the inverse Fourier transform to obtain a clear image without the "noise" present in the original micrographs.

### Results

#### Inclusion morphology and staining properties of clinical isolates of *C. pneumoniae*

The inclusions of KKpn-1, KKpn-15, KKpn-16 and other 15 clinical isolates positively stained with *C. pneumoniae*-specific MAbs and the genus-specific MAb (Cultureset), but not with *C. trachomatis*-specific MAb (MicroTrak) or iodine stain. Their morphology in HeLa 229 cells closely resembled that of *C. psittaci* and *C. pecorum*, which are oval and dense in the early stages in the Giemsa staining preparations. The inclusions expanded without compression of the host nucleus. These properties of the 18 clinical isolates obtained in our laboratory were identical with those of TWAR strains, indicating they are the members of the species *C. pneumoniae*.

#### Morphology of *C. pneumoniae* EBs in thin sections and shadowcast preparations

The chlamydial bodies in *in situ* inclusions of the

*C. pneumoniae* strains at 60 h postinoculation are shown in Fig. 1<sup>11, 14, 18, 32</sup>. A number of EBs and RBs are seen in the inclusions. There were no distinct differences in the RB morphology of the different strains. The EBs of KKpn-1, KKpn-15, KKpn-16, IOL-207, Kajaani-6, YK-41, and the 15 clinical isolates (Fig. 1a), however, were round<sup>11, 14, 17, 18, 32-34</sup> and their morphology was identical to that of *C. pecorum*, *C. psittaci*, and *C. trachomatis* EBs<sup>11, 14, 18, 27, 32</sup>. In contrast, the EBs of the TWAR strains had a wide

periplasmic space limited by a wavy outer membrane, creating "pear-shaped" profiles<sup>14, 18, 32, 35</sup> (Fig. 1b). A similar morphological difference between TWAR and other strains was seen when the purified EBs were dried in air and shadowcast (Fig. 2). The EBs of *C. pecorum*, *C. psittaci* and *C. trachomatis* strains had a round "fried egg" shape that was indistinguishable from the EBs of strains KKpn-1, KKpn-15, KKpn-16, IOL-207, Kajaani-6, YK-41, and the 15 clinical isolates<sup>14, 18, 32, 33</sup> (Fig. 2a). However, the EBs of

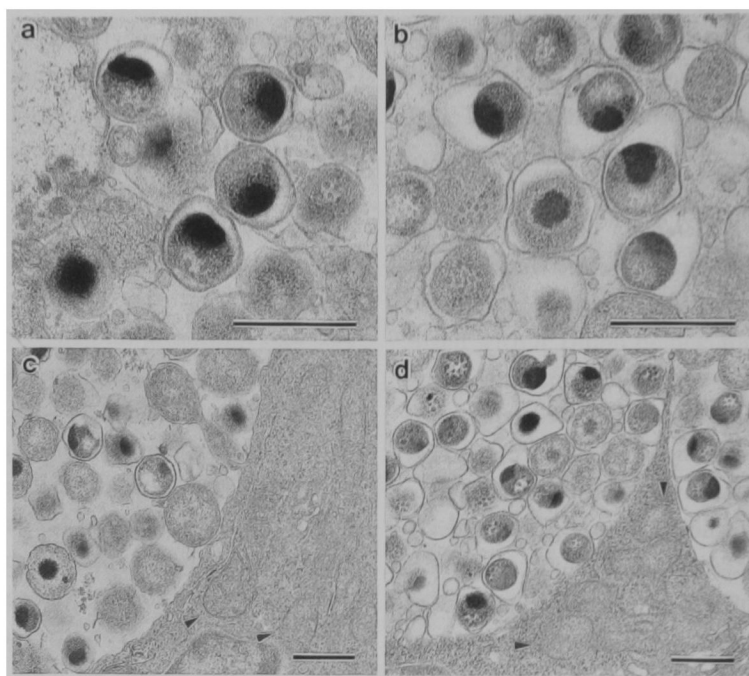


Fig. 1. Thin sections of KKpn-15 and AR-39 strains in HeLa 299 cells at 60 h postinoculation. a, *Chlamydia pneumoniae* KKpn-15; b, *C. pneumoniae* AR-39 at higher magnification. KKpn-15 EBs have a narrow periplasmic space and are round in shape, whereas AR-39 EBs are enclosed by a wavy outer membrane and are "pear-shaped" in profile. c, KKpn-15 inclusion. d, AR-39 inclusion. Arrowheads point to mitochondria located close to inclusions, but unassociated with the inclusion membrane. Bars; 500 nm.

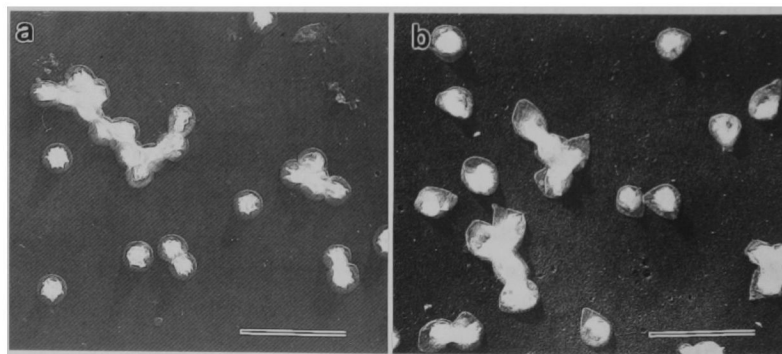


Fig. 2. Shadowcast of purified EBs of *Chlamydia pneumoniae* KKpn-15 (a) and TW-183 (b) strains. EBs were air-dried on a smooth-surfaced agar plate, transferred to a specimen grid by the pseudoreplica method with collodion, and then shadowcast with Pt-palladium alloy. Bars; 1  $\mu$ m.

the TWAR strains exhibited the "pear-shaped" morphology with a wide outer-membrane area even by the air-drying method (Fig. 2b).

Further observations on the distribution of mitochondria in the host cells infected with all strains of *C. pneumoniae* revealed the absence of any mitochondrial association with the inclusion membrane<sup>11, 14, 18, 27, 32</sup> (Fig. 1c, 1d arrowheads). This strongly suggested that the absence of the mitochondria-inclusion association is common in *C. pneumoniae* multiplication, although mitochondrial association with *C. psittaci* inclusions is a natural occurrence during the reproductive stage<sup>27</sup>.

### Surface projections and related structures

To examine the EB envelope and inclusion membrane, freeze-replicas of the inclusion-bearing cells were prepared at 60 h postinoculation. As shown in Fig. 3, the cleaved faces of the EBs and RBs were exposed as convex or concave faces in the replica membrane. Button structures (B structures)<sup>29</sup> or craters<sup>36</sup> were clearly seen in a limited area of the concave faces<sup>18, 32</sup> (Fig. 3, arrowheads). When the inclusion membrane was replicated, many fine particles grouped together within several areas were frequently observed on the convex faces<sup>18, 32</sup> (Fig. 4, arrowheads). The morphological properties of the B structures on the concave faces of *in situ* chlamydial bodies and the particles on the convex faces of inclusion membrane were identical with those mentioned previously<sup>4</sup>. Therefore, the results obtained in the present study strongly suggested the presence of projections on the surface of the *C. pneumoniae* EBs and

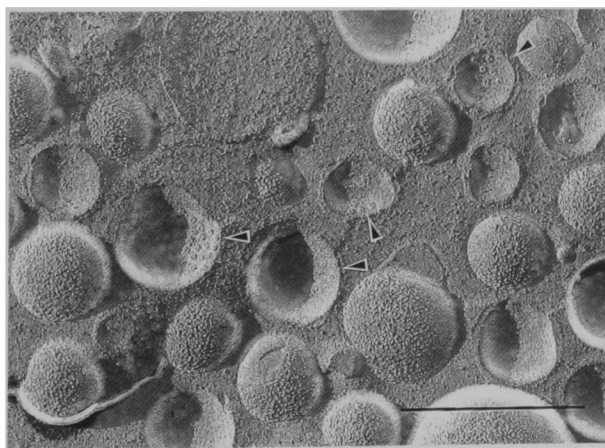


Fig. 3. Freeze-replica images of *in situ* chlamydial bodies and inclusion membranes of strain KKpn-15 at 60 h postinoculation. Chlamydial bodies are cleaved into convex or concave faces. Many B structures are seen (arrowheads). Bar; 1  $\mu$ m.

RBs.

To directly confirm the presence of projections on the surface of *C. pneumoniae* EBs, purified EBs were dried by the critical point drying method and examined by scanning electron microscopy<sup>18, 32</sup>. Projections were observed on a limited area of the EB surface of the *C. pneumoniae* strains<sup>18, 32</sup> (Fig. 5). The EBs of KKpn-15 were globular in shape (Fig. 5a), whereas those of the TWAR strains (Fig. 5b) had irregular shapes as a result of the presence of a wide periplasmic space. The number of projections on the EBs of each of the strains was not determined.

### Regular structure in the outer membranes

In a preliminary experiment, it was found that the

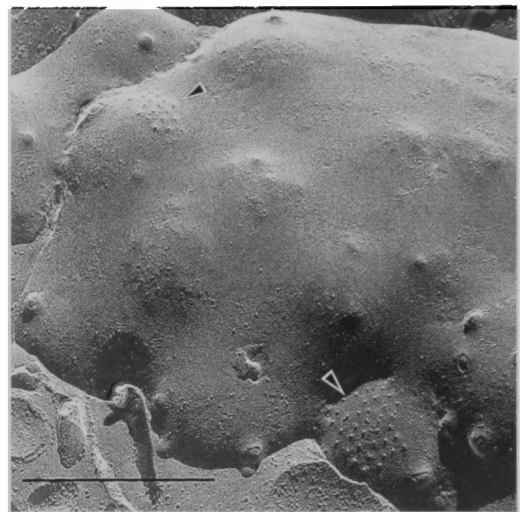


Fig. 4. Freeze-replica images of an *in situ* chlamydial inclusion membrane containing strain KKpn-15 at 60 h postinoculation. Fine particles in groups are indicated by arrowheads. The face is rugged over the RB outlines. Bar; 1  $\mu$ m.

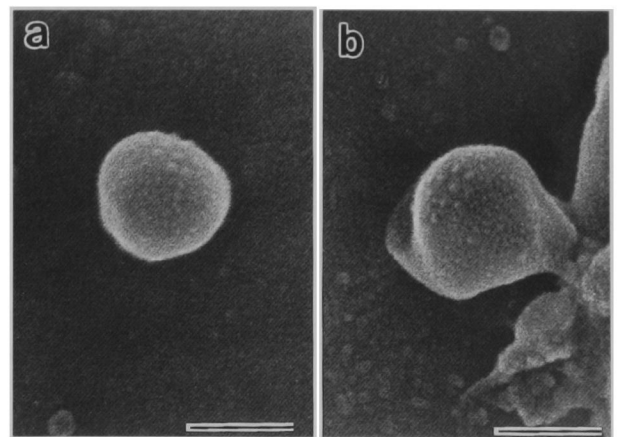


Fig. 5. Scanning electron micrograph of EBs of *Chlamydia pneumoniae* KKpn-15 (a) and AR-39 (b). Both micrographs show hexagonally arrayed projections in a limited area of the surface. Bars; 300 nm.

EB outer membranes of *C. pneumoniae* strains broke into small fragments when their envelopes were treated with 0.5% SDS to remove the inner membrane, whereas those of *C. psittaci* and *C. trachomatis* strains did not. This suggested that the outer membrane of *C. pneumoniae* EBs is fragile in SDS solution. Therefore, the SDS concentration was reduced from 0.5% to 0.125% to isolate the outer membranes of *C. pneumoniae*.

When the outer membranes were negatively stained, the hexagonally arrayed structures were clearly seen despite the difference in chlamydial species<sup>18, 32</sup> (Fig. 6). The dimensions of the structures appeared to be similar in all strains examined. Such regular structures were also seen in the shadowcast preparations only on the inner surface exposed by disintegration of the outer membrane (data not shown). These results were in good agreement with those reported previously<sup>17</sup>, indicating that the inner surface of the EB outer membrane of *C. pneumoniae* strains is also composed of hexagonally arrayed structures.

A computer Fourier transform was carried out<sup>18</sup> to determine the spacing of the hexagonal structure. Fig. 7 shows an example. As a result of the Fourier transform, the fragment of the KKpn-15 outer membrane shown in Fig. 6a yielded the diffraction spots in Fig. 7a. The spots show three different structural units of about 176, 90 and 50Å, respectively. When reconstruction by the inverse Fourier transform was performed for the innermost spots (176Å), a clear hexagonal pattern was obtained (Fig. 7b), and the periodicity in the outer membrane of all strains used

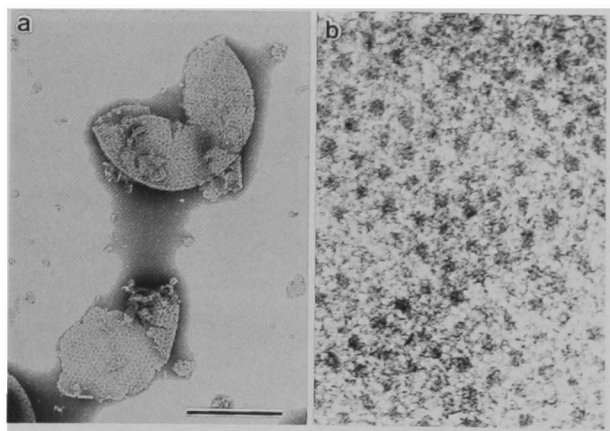


Fig. 6. Negatively stained EB outer membrane of *Chlamydia pneumoniae* KKpn-15 strain. b, higher magnification of the micrograph in a. The hexagonal structures are seen throughout the outer membrane. Bar; 200 nm.

in the present study was measured in this manner. The results are summarized in Table 1. The average periodicity of all strains was very similar despite the difference in morphology, i. e., the round or pear-shaped profile, in thin sections<sup>11, 14, 18, 32</sup>. These results indicate that the regular structure composing the inner layer of the EB outer membrane is a morphological property common to the EB outer membranes of the genus *Chlamydia*, although the outer membranes of the TWAR EBs show peculiar profiles in thin sections.

#### Immunolabeling of LPS on EBs and the diversity of the LPS of *C. pneumoniae*

When immunogold-labeling with anti-LPS MAb was carried out, the surface of the EBs of all chlamydial strains was heavily labeled with protein A-gold particles (Fig. 8). This finding indicated that the immunogold-labeling method was accurate and that the LPS was located on the EB surface.

The IDEIA chlamydia (DAKO Diagnostics Co.)<sup>26</sup> test kit is designed to detect *C. trachomatis* LPS,

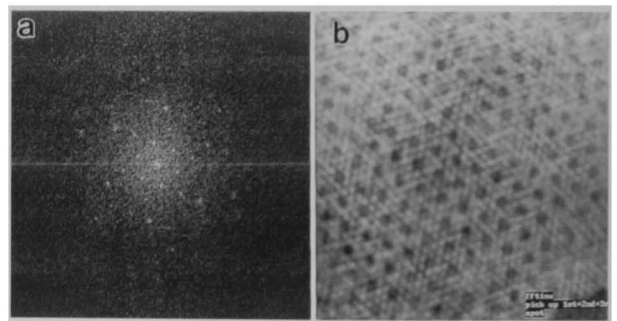


Fig. 7. Image processing of the hexagonal structures in the outer membrane of strain KKpn-15 EB. a, Diffraction spots obtained by Fourier transformation from the original micrograph shown in Fig. 6b; b, Image reconstituted by inverse Fourier transformation from the six spots of the diffraction shown in Fig. 7a.

Table 1. Comparison of periodicity in chlamydial species\*

Species	Strain	Mean periodicity $\pm$ SD
<i>C. pneumoniae</i>	round-shape	
	KKpn-15	179 $\pm$ 8 Å
	KKpn-16	178 $\pm$ 8 Å
	KKpn-1	176 $\pm$ 7 Å
	IOL-207	177 $\pm$ 7 Å
	Kajaani-6	178 $\pm$ 6 Å
	YK-41	176 $\pm$ 8 Å
pear-shape	TW-183	173 $\pm$ 7 Å
	AR-39	174 $\pm$ 8 Å
	AR-388	173 $\pm$ 8 Å
<i>C. trachomatis</i>	L2/434/Bu	176 $\pm$ 7 Å
<i>C. psittaci</i>	Frt-Hu/Cal 10	175 $\pm$ 8 Å

\* Periodicity measured from center to center by Fourier transform

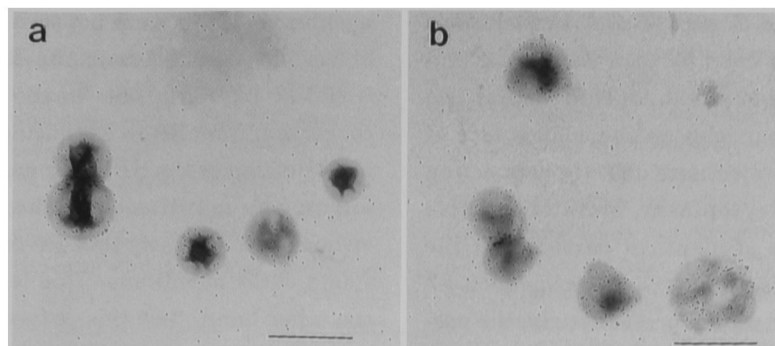


Fig. 8. Immunogold-labeling on the surface of EBs of the *Chlamydia pneumoniae* KKpn-15 (a) and TW-183 (b) strains. The samples were treated with monoclonal antibody directed to *Chlamydia psittaci* LPS, and then labeled with protein A-gold particles. Intact EBs and EB envelopes are heavily labeled with the protein A-gold particles. Bars; 500 nm.

Table 2. Diversity of *Chlamydia pneumoniae* strains in reaction intensity to the IDEIA test kit\*

Strain	Shape of EB	EB number per assay
IOL-207	round	$6.0 \times 10^4$
TW-183	pear-shape	$7.0 \times 10^4$
AR-388	pear-shape	$8.4 \times 10^4$
Kajaani-6	round	$1.2 \times 10^4$
AR-39	pear-shape	$2.4 \times 10^4$
KKpn-1	round	$2.8 \times 10^4$
YK-41	round	$4.0 \times 10^4$

\* The numbers of EBs are shown in increasing order

which is a major genus-specific (genus-common) antigen, and consequently the LPS of *C. psittaci* and *C. pneumoniae* also reacts with the IDEIA kit<sup>26</sup>. When the IDEIA kit was tested with particle number of purified *C. pneumoniae* EBs as a parameter, the reaction occurred positively at different intensities. No correlation was found between reaction intensity and EB morphology<sup>33</sup> (Table 2). However, it was not clarified whether the different reactivities of *C. pneumoniae* strains resulted from differences in the quality or quantity of LPS on the EB surface, although the chemical structure of the antigenic epitope in LPS has been proposed.

### Discussion

The morphology of *C. pneumoniae* TWAR strains was compared with that of *C. trachomatis* L2 and *C. psittaci* Cal 10. The TWAR EBs were shown to be "pear-shaped", with a large periplasmic space, in thin sections<sup>35</sup>, whereas those of *C. trachomatis* and *C. psittaci* were observed to be round. This morphological difference was confirmed again in the present study. However, the EBs of KKpn-1~18 and YK-41 strains, which were recognized as *C. pneumoniae* on

the basis of their properties, including reactivity with *C. pneumoniae*-specific MAbs and stainability with iodine, were found to have a narrow periplasmic space in sections and shadowcast preparations<sup>11, 14, 16, 32</sup>. Carter et al.<sup>34</sup> demonstrated that the EB morphology of *C. pneumoniae* IOL-207 strain was also round in thin sections and indistinguishable from that of *C. trachomatis* and *C. psittaci* EBs. Similarly, Popov et al.<sup>17</sup> demonstrated round EBs of *C. pneumoniae* Kajaani-6 strain. These results, together with the results obtained in the present study, strongly suggest that the "pear-shape" profiles of EBs in thin sections are not common among *C. pneumoniae* strains, and thus that the pear-shape is not valid as a morphological criterion for identifying *C. pneumoniae* species.

Based on a series of electron-microscopic studies on *C. psittaci* EBs, Matsumoto proposed a possible diagram showing the projections grouped together within a limited surface area and their related internal structures<sup>4</sup>. In a scanning electron microscopy study, Gregory et al.<sup>38</sup> and Matsumoto et al.<sup>39</sup> found the presence of projections on the EBs of many strains of *C. trachomatis* and *C. psittaci*, and in our study, scanning electron microscopy showed projections not only on TWAR EBs but on KKpn-1, KKpn-15, KKpn-16, and YK-41 EBs as well. Moreover, the presence of B structures<sup>29</sup> or craters<sup>36</sup> on the concave face of EBs in freeze replicas strongly suggests that the projections are common to all members of the genus *Chlamydia*, thereby supporting the proposition by Gregory et al.<sup>38</sup> that the projections are a phenotypic marker for recognizing members of the genus *Chlamydia*.

Matsumoto examined *C. psittaci* Cal 10 inclusions isolated from infected cells by thin sectioning and freeze-replica techniques and concluded that the hexagonally arrayed particles on the convex face of the inclusions were projections directly connecting the RBs to the host cytoplasm. Matsumoto also reported the presence of identical particles on the convex face of *in situ* inclusions of *C. trachomatis* L2 and *C. psittaci* strains<sup>41</sup>. In the present study, the particles were again seen on the convex face of the replicated inclusions of *C. pneumoniae* strains. It is, therefore, very likely that the RBs of *C. pneumoniae* strains also possess projections and that the direct connection between RBs and inclusion membranes with the projections is a common phenomenon during multiplication of the genus *Chlamydia*.

Matsumoto examined the outer membranes of *C. psittaci* EBs and reported that the dimensions of the hexagonal structures had a periodicity of 167Å by an optical transformation method using laser beams. However, in the present study, the periodicity in the Cal 10 outer membranes was estimated to be 175Å by the Fourier transform in the computer system. This difference (approximately 5%) appeared to be due to the difference in methods of measurement and seemed unavoidable. It was noteworthy that the EBs of the *C. pneumoniae* strains examined possessed hexagonal structures in the inner surface of the outer membrane and that no marked difference in periodicity was recognized between the round-shaped EBs (KKpn-1, KKpn-15, KKpn-16, IOL-207, Kajaani-6, YK-14) and the pear-shaped EBs (TW-183, AR-39 and AR-388). Based on these findings, it is very likely that the hexagonal structure composing the inner layer of the EB outer membrane is a morphological property common to the genus *Chlamydia*, although the outer membranes of the TWAR EBs show pear-shaped profiles. On the basis of a comparative study of EB and RB of *C. psittaci* Cal 10 strain, Matsumoto and Manire<sup>37</sup> suggested a correlation between the presence of hexagonal structures and the rigidity of the chlamydial bodies. In addition, outer membranes obtained from abnormal, giant RBs formed in the presence of penicillin<sup>41</sup> were also fragile and defective in the hexagonal structure<sup>42</sup>. Routine observations on the multiplication of many chlamydial strains with round EBs, such as *C. psittaci* and *C. trachomatis*, suggest that a large RB outer membrane may be diminished in size into a small EB outer

membrane. If this were not so, a number of fragments or vesicles derived from the RB outer membranes would be regularly seen in the inclusion during the conversion from RB to EB during maturation. A similar reduction of the RB outer membrane should occur during the maturation of the KKpn-1~KKpn-18 strains, because their EBs are enclosed tightly with a round outer membrane. This led us to speculate, on the other hand, that this reduction in size of the RB outer membrane is incomplete in the strains with pear-shaped EBs, such as *C. pneumoniae* TWAR. Thus, the relationship between the formation of the hexagonal structure and the reduction in size of the RB outer membrane is still unclear.

No mitochondria associated with the inclusion-containing *C. pneumoniae* strains used were detected. This finding is in good agreement with the results reported previously<sup>47</sup>. Therefore, it is likely that the absence of the mitochondria/inclusion association is also a common phenomenon in *C. pneumoniae* species.

*C. pneumoniae* was classified in 1989 as a new species on the basis of EB morphology, serology, and DNA analysis of the TWAR strains<sup>11</sup>. Since then, several *C. pneumoniae* strains, including our isolates, have been established from patients with respiratory diseases. It is noteworthy that in spite of the striking difference in EB morphology, only one serotype has been identified<sup>11</sup>. Although humans have been thought to be the natural reservoir of *C. pneumoniae*, similar chlamydiae have been isolated from a horse<sup>48</sup> and koala bear<sup>49</sup>. These findings, together with the variety of reactivity of many *C. pneumoniae* isolates in the IDEIA kit led us to speculate that different *C. pneumoniae* serotypes exist.

#### Acknowledgments

The authors wish to thank Uehira K, Suda T and Yamane K, Electron Microscope Center, Ohmori S and Tanaka Y, Department of Microbiology, and Nakabayashi M, Division of Respiratory Diseases, Department of Medicine, Kawasaki Medical School for their technical assistance. This work was supported by Project Research Grants #3-507, #4-504, #5-503 and #6-506 from Kawasaki Medical School and a Science Research Grant (04771177) from the Ministry of Education, Science and Culture, Japan.

#### Literature Cited

- 1) Grayston J T, Kuo C-C, Campbell L A, et al.: *Chlamydia pneumoniae* sp. nov. for *Chlamydia* sp. strain TWAR. Int J Syst Bacteriol 39: 88~90, 1989

- 2) Moulder J W, Hatch T P, Kuo C-C, et al.: *Chlamydia* Jones, Rake and Stearns 1945, 55, In Krieg NR (ed.), p. 729~739, Bergey's Manual of Systematic Bacteriology, Vol. 1. The Williams and Wilkins Co., Baltimore., 1984
- 3) Fukushi H, Hirai K: Proposal of *Chlamydia pecorum* sp. nov. for *Chlamydia* strains derived from ruminants. Int J Syst Bacteriol 42: 306~308, 1992
- 4) Matsumoto A: Structural characteristics of chlamydial bodies. In Barron A L (ed.), p.21~45, Microbiology of Chlamydia, Florida, U. S. A., CRC Press, 1988
- 5) Marrie T J: Community-acquired pneumonia. Clin Infect Dis 18: 501~515, 1994
- 6) Grayston J T, Wang S-P, Kuo C-C, et al.: Current knowledge on *Chlamydia pneumoniae*, strain TWAR, an important cause of pneumonia and other acute respiratory disease. Eur J Clin Microbiol Infect Dis 8: 191~202, 1989
- 7) Grayston J T, Kuo C-C, Wang S-P, Altman J: A new *Chlamydia psittaci* strain, TWAR, isolation in acute respiratory tract infections. N Engl J Med 315: 161~168, 1986
- 8) Saikku P, Leinonen M, Tenkanen L, et al.: Chronic *Chlamydia pneumoniae* infection as a risk factor for coronary heart disease in the Helsinki Heart Study. Ann Intern Med 116: 273~278, 1992
- 9) Kuo C-C, Shor A, Campbell L A, et al.: Demonstration of *Chlamydia pneumoniae* in atherosclerotic lesions of coronary arteries. J Infect Dis 167: 841~849, 1993
- 10) Blasi F, Legnani D, Lombardo V M, et al.: *Chlamydia pneumoniae* infection in acute exacerbations of COPD. Eur Respir J 6: 19~22, 1993
- 11) Miyashita N, Matsumoto A, Kubota Y, et al.: Continuous isolation and characterization of *Chlamydia pneumoniae* from a patient with diffuse panbronchiolitis. Microbiol Immunol 40: 547~552, 1996
- 12) Hahn D L, Dodge R W, Golubjatnikov R: Association of *Chlamydia pneumoniae* (strain TWAR) infection with wheezing, asthmatic bronchitis, and adult-onset asthma. JAMA 266: 225~230, 1991
- 13) Hahn D L, Golubjatnikov R: Asthma and chlamydial infection: a case series. J Fam Pract 38: 589~595, 1994
- 14) Miyashita N, Kubota Y, Kimura M, et al.: Characterization of a *Chlamydia pneumoniae* strain isolated from a 57-year-old man. Microbiol Immunol 38: 857~864, 1994
- 15) Kishimoto T, Soejima R: Current topics of chlamydial respiratory tract infections-special reference to the epidemiology and clinical findings of *Chlamydia pneumoniae* infections in Japan. Intern Med 32: 934~937, 1993
- 16) Dwyer R St C, Treharne J D, Jones B R, et al.: Chlamydial infection: Results of micro-immunofluorescence tests for the detection of type-specific antibody in certain chlamydial infections. Br J Vener Dis 48: 452~459, 1972
- 17) Popov V L, Shatkin A A, Pankratova V N, et al.: Ultrastructure of *Chlamydia pneumoniae* in cell culture. FEMS Microbiol Lett 84: 129~134, 1991
- 18) Miyashita N, Kanamoto Y, Matsumoto A: The morphology of *Chlamydia pneumoniae*. J Med Microbiol 38: 418~425, 1993
- 19) Francis T Jr, Magill T P: An unidentified virus producing acute meningitis and pneumonitis in experimental animals. J Exp Med 68: 147~163, 1938
- 20) Schachter J, Meyer K F: Lymphogranuloma venereum. II. Characterization of some recently isolated strains. J Bacteriol 99: 636~638, 1969
- 21) McNutt S H, Waller E F: Sporadic bovine encephalomyelitis (Buss disease). Conell Vet 30: 437~448, 1940
- 22) Kuo C-C, Chen H-H, Wang S-P, et al.: Identification of a new group of *Chlamydia psittaci* strains called TWAR. J Clin Microbiol 24: 1034~1037, 1986
- 23) Iijima Y, Miyashita N, Kishimoto T, et al.: Characterization of *Chlamydia pneumoniae* species-specific proteins immunodominant in humans. J Clin Microbiol 32: 583~588, 1994
- 24) Tamura A, Higashi N: Purification and chemical composition of meningopneumonitis virus. Virology 20: 596~604, 1963
- 25) Caldwell H D, Kromhout J, Schachter J: Purification and partial characterization of the major outer membrane protein of *Chlamydia trachomatis*. Infect Immun 31: 1161~1176, 1981
- 26) Miyashita N, Matsumoto A: Establishment of a particle-counting method for purified elementary bodies of chlamydiae and evaluation of sensitivities of the IDEIA Chlamydia kit and DNA probe by using the purified elementary bodies. J Clin Microbiol 30: 2911~2916, 1992
- 27) Matsumoto A, Bessho H, Uehira K, et al.: Morphological studies of the association of mitochondria with chlamydial inclusions and the fusion of chlamydial inclusions. J Electron Microsc 40: 356~363, 1991
- 28) Matsumoto A, Higashi N, Tamura A: Electron microscope observations on the effects of polymixin B sulfate on cell walls of *Chlamydia psittaci*. J Bacteriol 113: 357~364, 1973
- 29) Matsumoto A: Fine structures of the cell envelopes of *Chlamydia* organisms as revealed by freeze-etching and negative staining techniques. J Bacteriol 116: 1355~1363, 1973
- 30) Matsumoto A: Electron microscopic observations of surface projections and related intracellular structures of *Chlamydia* organisms. J Electron Microsc 30: 315~320, 1981
- 31) Birkelund S, Lundemose A G, Christiansen G: Immunoelectron microscopy of lipopolysaccharide in *Chlamydia trachomatis*. Infect Immun 57: 3520~3523, 1989
- 32) Miyashita N, Matsumoto A: Microbiology of chlamydiae - with emphasis on physicochemistry, antigenicity and drug susceptibility of *Chlamydia pneumoniae* - . Kawasaki Med J 20: 1~17, 1994

- 33) Miyashita N, Kishimoto T, Soejima R, et al.: Reactivity of *Chlamydia pneumoniae* strains in the IDEIA CHLAMYDIA test kit designed for detection of *Chlamydia trachomatis*. Jpn J Associ Infect Dis 67: 549~555, 1993
- 34) Carter M W, Al-Mahdawi S A H, Giles I G, et al.: Nucleotide sequence and taxonomic value of the major outer membrane protein gene of *Chlamydia pneumoniae* IOL-207. J Gen Microbiol 137: 465~475, 1991
- 35) Chi E Y, Kuo C-C, Grayston J T: Unique ultra-structure in the elementary body of *Chlamydia sp.* strain TWAR. J Bacteriol 169: 3757~3763, 1987
- 36) Louis C, Nicolas H, Eb F, et al.: Modification of the envelope of *Chlamydia psittaci* during its developmental cycle: freeze-fraction study of complementary replica. J Bacteriol 141: 868~875, 1980
- 37) Matsumoto A, Manire G P: Electron microscopic observations on the fine structure of cell walls of *Chlamydia psittaci*. J Bacteriol 104: 1332~1337, 1970
- 38) Gregory W W, Gardner M, Byrne G I, et al.: Arrays of hemispheric surface projections on *Chlamydia psittaci* and *Chlamydia trachomatis* observed by scanning electron microscopy. J Bacteriol 138: 241~244, 1979
- 39) Matsumoto A, Bessho H: Surface projections of elementary bodies of *Chlamydia* strains in electron microscopy 1986 (Imura T, Maruse S, Suzuki T, eds), Marzen, Tokyo, 3349~3350, 1986
- 40) Matsumoto A: Isolation and electron microscopic observations of intracytoplasmic inclusions containing *Chlamydia psittaci*. J Bacteriol 145: 605~612, 1981
- 41) Tamura A, Manire G P: Effect of penicillin on the multiplication of meningo-pneumonitis organisms (*Chlamydia psittaci*). J Bacteriol 96: 875~880, 1968
- 42) Matsumoto A, Manire G P: Electron microscopic observations on the effect of penicillin on the morphology of *Chlamydia psittaci*. J Bacteriol 101: 278~285, 1970
- 43) Storey G, Lusher M, Yates P, et al.: Evidence for *Chlamydia pneumoniae* of non-human origin. J Gen Microbiol 139: 2621~2626, 1993
- 44) Kaltenboeck B, Kousoulas K G, Storz J: Structures and allelic diversity and relationships among the major outer membrane protein (ompA) genes of the four chlamydial species. J Bacteriol 175: 487~502, 1993

### *Chlamydia pneumoniae* の形態学的解析

宮下 修行<sup>1)\*\*</sup>・松本 明<sup>2)</sup>・副島 林造<sup>3)</sup>・岸本 寿男<sup>1)</sup>

中島 正光<sup>1)</sup>・二木 芳人<sup>1)</sup>・松島 敏春<sup>1)</sup>

<sup>1)</sup>川崎医科大学呼吸器内科\*, <sup>2)</sup>同 微生物学教室

<sup>3)</sup>川崎医療福祉大学医療福祉学科

*Chlamydia pneumoniae* は 1989 年に新種となったクラミジアであり、従来その分離培養は困難とされていた。最近我々は、急性呼吸器感染症患者の咽頭スワブから計 18 株の分離に成功した (KKpn-1 から KKpn-18 と命名)。今回これら臨床分離 18 株を中心に超微構造を、既存の *C. pneumoniae* TW-183, AR-39, AR-388 (以上 TWAR 株), IOL-207, Kajaani-6, YK-41 株, *Chlamydia psittaci* Frt-Hu/Cal 10 株, *Chlamydia trachomatis* L2/434/Bu 株ならびに *Chlamydia pecorum* Bo/E58 株と比較検討した。TWAR 株の基本小体 (elementary body; EB) は、広い periplasmic space をもつ西洋梨状を呈し、*C. pneumoniae* を新種としたクライテリアの 1 つとして挙げられている。しかし、今回対象とした KKpn-1 ~ KKpn-18 株 EB は円形で *C. psittaci*, *C. trachomatis*, *C. pecorum* の EB 同様に狭い periplasmic space を有していた。また同様に IOL-207, Kajaani-6, YK-41 株 EB も円形であったことから、EB の広い periplasmic space は *C. pneumoniae* の形態学的特徴とはいえないことが判明した。しかし、クラミジア独特の表面突起 (surface projection; SP) および B 構造、封入体膜上の SP 集団が用いたクラミジア全株に認められ、EB の基本形態に差がないことが判明した。したがって *C. psittaci*, *C. trachomatis* 同様 SP を介する host-*Chlamydia* interaction のあることが示唆された。EB の剛性は外膜に依存していると考えられており、*C. psittaci*, *C. trachomatis* の外膜内面は hexagonal な規則的構造 (hexagonal structure; HS) で形成され、脆弱な網様体 (reticulate body; RB) 外膜には HS がいないことから、この HS と剛性の間の相関性が強く示唆されている。TWAR 株の EB が西洋梨状を呈していることや、超音波処理・界面活性剤 (SDS) 処理に対する脆弱性・感受性が異なることから HS に相違がみられると予想されたが、いずれの株においても HS が認められ、その周期性は種間、株間で有意差はなかった。

\*岡山県倉敷市松島 577

\*\*現住所 (連絡先): 4717 24th Ave. N.E. #334, Seattle, Washington 98105, USA Phone/Fax (206)-729-1385